Bioprocess Biosyst Eng (2017) 40:1813–1823
DOI 10.1007/s00449-017-1835-6

RESEARCH PAPER

Biomechanical properties and cellular biocompatibility of 3D printed tracheal graft

Yibo Shan[1,2,3] · Yao Wang[1,2,3] · Jianfeng Li[1,2,3] · Hongcan Shi[1,2,3,4] · Yiwei Fan[1,2,3] · Junfeng Yang[1,2,3] · Weidong Ren[1,2,3] · Xi Yu[2,3]

Received: 29 March 2017 / Accepted: 30 August 2017 / Published online: 8 September 2017

Abstract The goals of our study were to evaluate the biomechanical properties and cellular biocompatibility of 3D printed tracheal graft fabricated by polycaprolactone (PCL). Compared with native tracheal patch, there was a significant increase in maximum stress and elastic modulus for 3DP tracheal graft ($p < 0.05$). BMSCs were co-cultured under four different conditions to investigate cytotoxicity of the graft: (1) co-cultured with normal culture medium, as blank control; (2) co-cultured with perfluoropropylene, as negative control; (3) co-cultured with 3DP tracheal graft; and (4) co-cultured with polyvinyl chloride, as positive control. Moreover, the results of SRB assay showed that compared with blank and negative control group, there was no significant difference in the cell proliferation of 3DP tracheal graft group for 21 days ($p > 0.05$). These results revealed that 3DP tracheal graft in our study has favorable cellular biocompatibility and biomechanical properties, and, therefore, will be a promising alternative for tissue-engineered trachea.

Keywords 3D printed tracheal graft · PCL · Biomechanical properties · Cellular biocompatibility · Tissue-engineered trachea

Introduction

Tracheal resection and end-to-end anastomosis has been the standard clinical approach for the treatment of most airway diseases which can result from stenosis, tracheomalacia, and tumors [1]. However, when the length of the diseased trachea exceeds more than one-half of the total length in adults or more than one-third of the total length in children, tracheal replacement or reconstruction seems to be the only possible solution [2, 3]. A matrix, used in tracheal replacement, should meet the basic tracheal characteristics: being bioactive, capable of enhancing tissue regeneration, nonimmunogenic, nontoxic, and noncarcinogenic/nonteratogenic [4]. The main modes of tracheal reconstruction include artificial tracheal transplantation, allogeneic transplantation and tissue engineering tracheal transplantation. Artificial tracheal transplantation usually causes rupture, infection and narrow of the trachea tissue, the most serious problem is lack of epithelization which leads to failure [5]. At the same time, allogeneic transplantation needs long-term immunosuppressive therapy, also the necrosis of implanted graft and postoperative infection which caused by inadequate vascular regeneration often lead to death [6]. Tissue engineering which introduces engineered tissue constructs for the regeneration of the desirable native tissue has distinct virtues, not only for supporting ex vivo cultured cells, but also serving as a carrier to deliver the appropriate signal and necessary nutrition to defective areas to help tissue regeneration [7, 8]. With 3D printing technology spread more and more

Yibo Shan and Yao Wang contributed equally to this work.

✉ Hongcan Shi
shihongcan@hotmail.com

[1] Department of Cardiothoracic Surgery, Clinical College of Yangzhou University, Yangzhou 225001, China

[2] Key Laboratory of Integrative Medicine in Geriatrics Control of Jiangsu Province, Yangzhou University, Yangzhou 225001, China

[3] Center of Translational Medicine, Yangzhou University, Yangzhou 225001, China

[4] College of Medicine, Yangzhou University, 11 Huaihai Road, Yangzhou 225001, China

wildly, it has been already used as an alternative strategy for tracheal reconstruction. The development of 3D printing provides a new train of thought to solve the problem of epithelization and vascularization.

Schantz compared differentiated cells (osteoblasts) and adult progenitor cells (mesenchymal progenitor cells, MPCs) in 2D culture and in combination with a computer-designed 3D porous scaffold using Fused Deposition Modeling(FDM) technology, in terms of their efficiency and efficacy in the repair of cranial bone defects in a rabbit model [9]. And the results showed that the combination of a mechanically stable synthetic framework (PCL scaffolds) and a biomimetic hydrogel (fibrin glue) provides a potential matrix for bone tissue-engineering applications. Chang used polycaprolactone (PCL) as material, combined with 3D-printed (3DP) scaffold which coated with mesenchymal stem cells (MSCs) seeded in fibrin to help repairing partial tracheal defects [10]. A half-pipe-shaped 3DP PCL scaffold was designed, fabricated and then implanted on a 10 × 10 mm artificial tracheal defect in four rabbits. Four and eight weeks after the operation, the reconstructed parts were evaluated bronchoscopically, radiologically, histologically, and functionally. The results did not show any sign of respiratory distress. In other words, the shape and function of reconstructed trachea using 3DP PCL scaffold coated with MSCs seeded in fibrin were restored successfully without any graft rejection. In general, 3D printing has come into the spotlight in the realm of tissue engineering. The purpose of our study was to use PCL as the material to print the tracheal scaffold through the 3D printing technology and to study its biomechanical properties and cellular compatibility. To find a suitable tissue engineering tracheal scaffold material.

Materials and methods

All the experiments were conducted in accordance with the Guidance suggestions of caring and using laboratory animals, issued by the Ministry of Science and Technology of the People's Republic of China in 2006. The study protocol complied with all committee regulations approved by the Ethics Committee of Medical College of Yangzhou University.

Design and fabrication of the 3D printed tracheal graft

The 3D printed (3DP) porous tracheal graft with a half-pipe shape (10 × 10 mm) was designed using Rhinoceros 5.0. The bio-printer (UN-3DBI-I01) was supported by Qingdao Unique Products Develop Co., Ltd (Qingdao, China). The fused deposition modeling (FDM) method extruding materials out of nozzles, which is able to move back and forth along the axis of rotation at a certain speed of 5 mm/s [11, 12]. The extruded strand was deposited onto a platform. Once the first layer of material was deposited, another layer was then delivered on top of the previous one at the crossed direction according to the designed specifications to form porous shape, and the process was repeated six times until the completion of the desired tracheal graft. Aperture of the tracheal graft can be adjusted by the speed of the axis of rotation and print head.

Fabrication of 3DP graft was done with PCL which were melted at 90 °C through a heated nozzle, and the strand of PCL was plotted as layer-by-layer deposition on a stage, as described above. The distance between strands was 0.3 mm. The thickness of the 3DP graft was 1 mm, and inner diameter was 6 mm which is comparable with the diameter of a normal rabbit trachea, and the pore size was made at 300 μm.

Scanning electron microscope (SEM) of 3DP tracheal grafts

The external and internal surface morphology of 3DP tracheal grafts coated with gold/palladium for 20 min were observed by scanning electron microscope (S4800, Hitachi, Tokyo, Japan) operated at 15 kV.

Mechanical test of the 3D printed tracheal graft

Native tracheas were acquired from six young New Zealand white rabbits (2.5–3.0 kg, 4 month old, female). The cervical trachea was exposed through a vertical skin incision. Split the sternohyoid and sternothyroid muscles along the medial line after anesthesia. The trachea was cutoff.

The length, width and thickness of each sample were measured using vernier caliper. A single-column Instron 3367 mechanical testing system (Instron, Norwood, USA) was used to investigate the mechanical behavior of each sample. Mechanical testing, including maximum stress and elastic modulus, was conducted at a velocity of 30 mm/min and a initial load of 1 N. Displacement was monitored in this process.

Isolation and culture of mesenchymal stem cells

Bone marrow mesenchymal stem cells (BMSCs) were isolated from tibial plateau with whole bone marrow adherent culture method under aseptic conditions. The rabbit was anesthetized with intramuscular injection of Xylazine hydrochloride (HuaMu animal health products co, Jilin province, China) at 0.2 ml/kg. Bone marrow puncture needles were used for puncture, and then bone marrow was aspirated for 2 ml with 5 ml syringe

containing heparin sodium already. The mixture of bone marrow and heparin sodium was injected into the 15 ml centrifuge tube (Corning, New York, USA). The mixture was centrifuged for 5 min at 1000 rpm (Labofuge 400R, Thermo Fisher, Germany) and supernatant was removed. Pellets were washed with phosphate-buffered saline (PBS) and centrifuged again. Cells were re-suspended with 10 ml culture medium consisting of 10% fetal bovine serum (FBS, Clark, USA) and 1% penicillin/streptomycin (Beyotime Biotechnology, Shang hai, China) in DMEM/F12 (HyClone, Utah, USA). The cell suspensions were transferred to 25 cm^2 cell culture flasks (Corning) and cultured in incubator (RS232, Thermo Fisher) at 37 °C, 5% CO_2. Through whole bone marrow adherent culture method, nonadherent cells were washed and the culture medium was changed after 48 h for the first time. Thereafter, the culture medium was replaced every 2 days and the cell growth was observed until cells were subcultured at 80% confluence. The culture medium was removed and then the cells were washed using PBS for two times. After that, cells were trypsinized by 2.5 g/l trysin (Gibco, New York, USA) at 1 ml and re-suspended. The above experiment was repeated to acquire 3rd passage BMSCs.

Identification of BMSCs

Morphologic observation

Cell shape and proliferation were observed daily with inverted phase contrast microscopy (CKX41SF, Olympus, Japan).

Immunofluorescence analysis

Immunofluorescence analysis was performed to identify BMSCs, as previously described [13, 14]. The sterilized glass was put into cell culture plate (Corning), and the 3rd passage cell suspensions were added on the glass through a dropper and cultured at 37 °C, 5% CO_2 for 12 h. Cells were fixed with 4% paraformaldehyde (Solarbio, Beijing, China) for 90 min, afterwards, cells were washed three times with PBS for 2 min each, incubated with 0.5% Triton X-100 (Sigma, St. Louis, USA) at 37 °C for 20 min, washed twice with PBS for 5 min each, blocked with 1% BSA (Sigma) at 37 °C for 30 min. Then unnecessary liquid was removed, and cells were incubated with anti-rabbit antibodies containing fluorescein: CD34-PE and CD44-PE (Bioss, Beijing, China), overnight at 4 °C, finally washed three times with PBS for 2 min each. Meanwhile, as a negative control, antibody was replaced with PBS. The distributions were observed with fluorescent microscopy (BX41TF, Olympus).

Adipogenic induction

Adipogenic induction experiment was performed with 3rd passage cells. Briefly, 0.5×10^5/ml cultured cells were seeded in 6-well plates (Corning) with DMEM/F12 (HyClone). When cells were subcultured at 80% confluence, BMSC medium was replaced with adipose medium, consisting of BMSC medium supplemented with 0.5 mM xanthine (Solarbio), 1 μM dexamethasone (Sigma), 10 μg/ml insulin (Sigma) and 70 μM indomethacin (Solarbio). The medium was replaced every 2 days. After 10 days, the medium was removed, and cells were washed three times with PBS for 5 min each, then, fixed with 4% paraformaldehyde (Solarbio) for 10 min, washed three times with PBS for 5 min each again, finally stained by Oil red O (Solarbio) for 10 min. The results were observed with inverted phase contrast microscopy (CKX41SF, Olympus).

In vitro biocompatibility testing of 3D printed tracheal graft

The toxicity of biological materials in our experiment refers to the International Standardization Organization (ISO 10993-1:1992).

Cellular morphology

This part of our experiment was divided into four groups: blank control group, perfluoropropylene group (negative control), 3DP tracheal patch group, polyvinyl chloride group (positive control). These tested materials were put into a cell culture plate, respectively, followed by the addition of 1 ml 3rd passage cell suspensions (1.0×10^5 cells/ml) and 1 ml BMSC medium. Moreover, each group repeated five times as parallel sample. All cells were cultured in incubator at 37 °C, 5% CO_2. Cellular morphology on the surface and the edge of materials were observed by inverted phase contrast microscopy (CKX41SF, Olympus), and toxicity grading scale was according to the morphology and growth status of cultured cells, as shown in Table 1.

SEM micrographs of cells adhered to the materials

BMSCs were co-cultured with 3DP tracheal graft for 7 days. Cells/graft was then immersed in 2.5% glutaraldehyde at 4 °C for 24 h. After that, cells/graft was washed three times with PBS for 10 min each. The cells/graft was coated with gold/palladium using a sputter coater for 20 min and was observed by SEM operated at 15 kV, after the progress of dehydration in 70, 80, 90, 95 and 100% ethanol one by one.

Table 1 Cellular morphology and toxicity grading scale

Grades	Cellular morphology and growth status
Non-toxic	Normal cellular morphology, adherent growth, fusiform /polygonal appearance
Mild	Adherent growth, but a few cell pyknosis, occasional suspension cells
Moderate	Poor adherent growth, cell pyknosis more than 30%, dead cells can be observed
Severe	Almost no adherent cells, more than 90% cells were dead

Identification of the cells in 3D printed tracheal graft

BMSCs were co-cultured with 3DP tracheal graft and the culture medium was replaced every 2 days. At day 10, the culture medium was removed and then the graft was rinsed with PBS for 2 times. After that, cells were trypsinized by 2.5 g/l trysin.

Flow cytometry was another method to confirm CD34 and CD44 expression. The cells were incubated with anti-CD34-PE, anti-CD44-PE for 30 min at 4 °C under the environment of darkness. Meanwhile, PBS was used as a negative control. Labeled cells were washed, collected, and analyzed using the flow cytometry system (BD, Franklin Lakes, USA).

Proliferation index of the cells

Sulforhodamine B (SRB) assay was used to measure cell proliferation. This part of our experiment was divided into four groups as described above. These tested materials were made at the size of 1 cm^2, and were immersion in 75% ethanol for 15 min, then exposed to a high-dose of UV light for 12 h to ensure adequate sterilization. Finally, the materials were dropped in 10 ml DMEM-F12 medium containing 10% FBS, shaking at 37 °C for 24 h. Thus, the dipping medium was obtained for the following experiment. 3rd passage cells were trypsinized and re-suspended with BMSC medium, subsequently counted and seeded at a density of 1.0×10^5 cells/ml in 96-wells plate. Each well has 100 µl cell suspension. All cells were cultured in incubator at 37 °C, 5% CO_2. After 24 h, the BMSC medium was replaced by the dipping medium which had been prepared above. The SRB assay was conducted at day 1, 3, 5, 7, 9. Optical density (OD) for the cell growth curve was valued by microplate reader (Epoch, BioTek, Vermont, USA).

Furthermore, the cells were co-cultured with blank control group, negative control group and 3DP tracheal graft for 21 days to investigate the longer stability of the 3DP graft.

Statistical analysis

All values were analyzed and tested with a commercial statistical software package (SPSS 19.0, Inc, Chicago, IL) and expressed as the mean ± standard deviation. Significant differences were analyzed by ANOVA followed by Student–Newman–Keuls *t* tests for post-hoc comparisons. Differences were considered significant at the 95% level ($p < 0.05$).

Results

3DP tracheal graft and morphological observations

Photograph and SEM images of the tracheal graft fabricated by the 3D printing technology were shown in Figs. 1 and 2. Two kinds of the size of the graft were fabricated successfully (Fig. 1). The SEM images revealed that the pore size was 300 µm for effective communication of cells (Fig. 2).

Biomechanical characteristics of native and 3DP tracheal graft

The mechanical behavior of the 3DP tracheal graft was significantly superior to native tracheal graft. Two mechanical properties of the material, maximum stress (*N*) and elastic modulus (mPa), were tested (Table 2). The time course of mechanical data of 3DP tracheal graft was shown in Fig. 3.

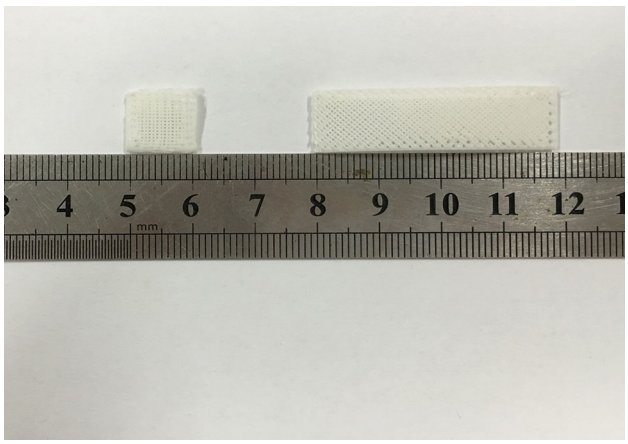

Fig. 1 The macroscopic structure of 3DP tracheal graft. The 3DP graft made with PCL was 10 mm × 10 mm (*left*) and 10 mm × 0 mm (*right*)

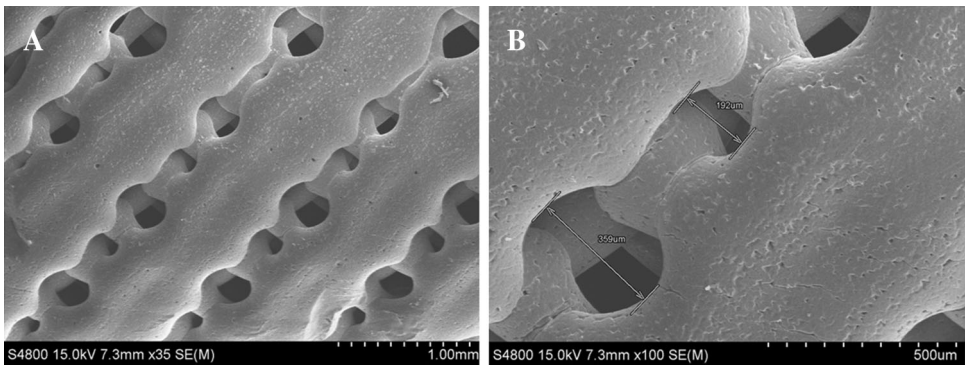

Fig. 2 SEM micrographs of the 3DP tracheal graft. **a** The graft had pore designs and interconnected pore networks (magnification ×35); **b** The pore size was varied from 200–400 μm (magnification ×100)

Table 2 The morphological and biomechanical characteristics of native and 3DP tracheal graft (mm, $n = 6$, $\overline{X} \pm s$)

Index	Native tracheal patch	3DP tracheal patch
Morphology		
Length (mm)	50.23 ± 0.31	50.33 ± 0.19
Width (mm)	11.50 ± 0.46	11.70 ± 0.17
Thickness (mm)	0.83 ± 0.06	1.13 ± 0.04
Mechanical behavior		
Maximum stress (N)	6.46 ± 0.92	58.16 ± 2.78[a]
Elastic modulus (mPa)	1.62 ± 0.13	93.27 ± 7.83[a]

Comparison with the native tracheal graft

[a] $p < 0.05$

Culturing and identification of BMSCs

Morphologic observation

BMSC has a characteristic of adherent, grows in clusters, shows different forms. Nonadherent cells were washed and fusiform adherent cells were obvious when the culture medium was changed after 48 h for the first time (Fig. 4a). After two replacements of culture medium, those impure cells including RBCs, platelets were cleared. Cellular morphology was varied: spindle-shaped cells, and polygonal, irregular, and unorganized cell colony were observed at day 6 (Fig. 4b). Cells reached 90% confluence at day 10 (Fig. 4c). More flat cells can be seen of 3rd passage BMSCs (Fig. 4d).

Analysis of immunophenotype

Immunofluorescent staining indicated that the CD44-PE cell marker fluoresced green on the surface of cells under a fluorescent microscope. CD34-PE fluoresced brown. In other words, cultured cells were positive for CD44 (Fig. 5a), but negative for CD34 (Fig. 5b).

Analysis of differentiation potential

BMSCs were treated with adipogenic inductor to differentiate into adipocytes. And the differentiated cells were identified by oil red O staining (Fig. 6).

In vitro biocompatibility testing of 3DP tracheal graft

Cell morphology observation

Cell morphology of 3DP tracheal graft group (Fig. 7c) was normal at days 1–7, cells grew adherently and were no significant difference with the blank control group (Fig. 7a) and the negative control group (Fig. 7b); at the same time, a large number of death cells were observed in positive control group (Fig. 7d); cells turned round and showed poor adherent growth; cell pyknosis and vacuoles were obvious.

SEM observation

BMSCs co-cultured in vitro on the 3DP tracheal graft were observed by SEM. The BMSCs were attached to the surface (Fig. 8a) and inside the pores of the 3DP tracheal graft after 7 days (Fig. 8b, c). BMSCs were found to attach onto the 3DP tracheal graft successfully and had a spread-out phenotype. The cells had a connection to adjacent cells and formed a fibrous network.

Identification of the cells

The expression of CD44 and CD34 for the cells in 3DP tracheal graft was examined by flow cytometry. The cells

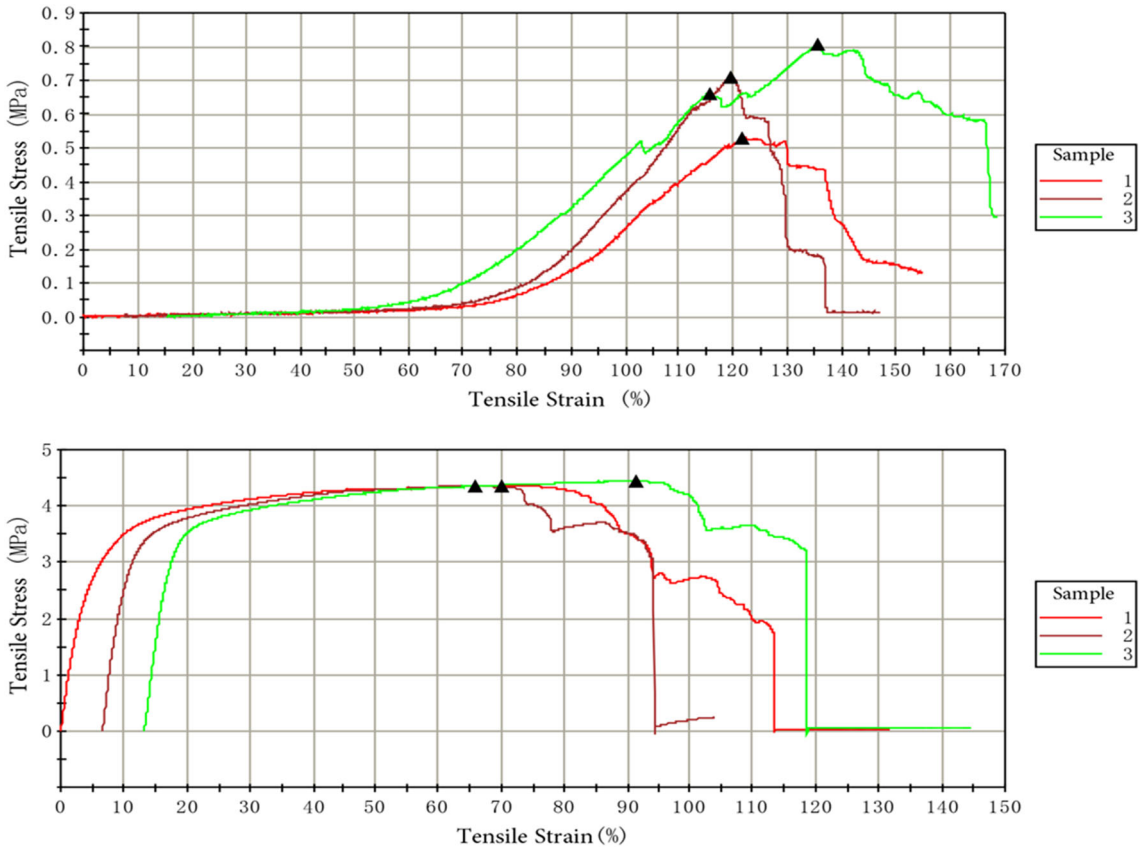

Fig. 3 The time course of mechanical data. The data of native tracheal patch was in the picture above and 3DP tracheal patch was in the picture below

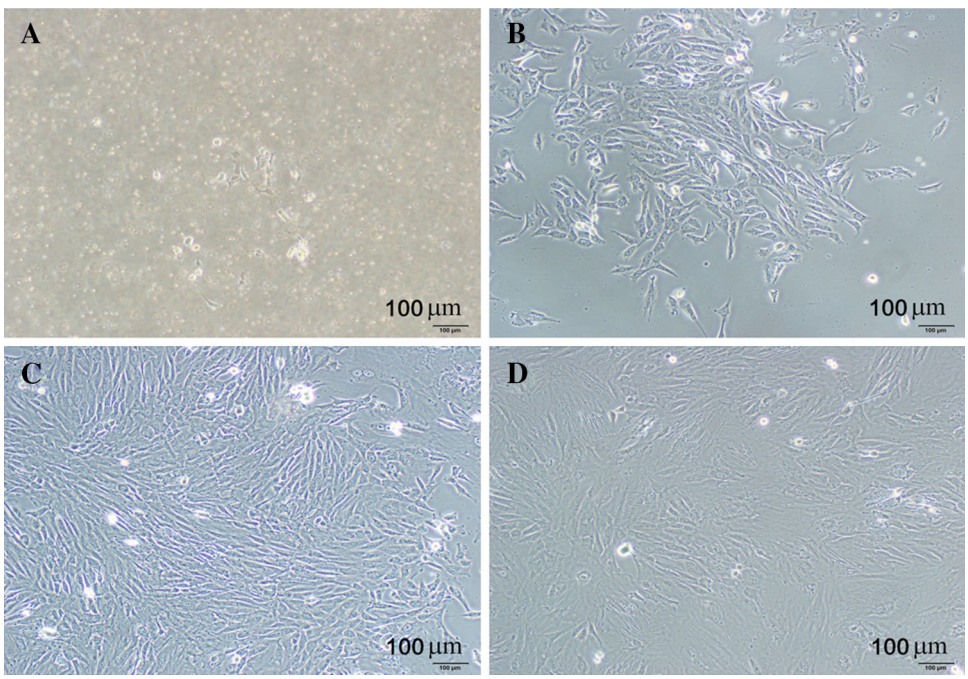

Fig. 4 Morphologic observation of BMSCs. RBCs were observed under inverted phase contrast microscopy after cells were seeded in cell culture flasks. **a** 48 h after culturing, adherent cells were obvious. **b** At day 6, no RBCs left and cells grew well and fast. **c** At day 10, cells can be passaged. **d** The 3rd passage BMSCs. The culture medium was replaced every 2 days. *Scale bar* 100 μm, applies to all images

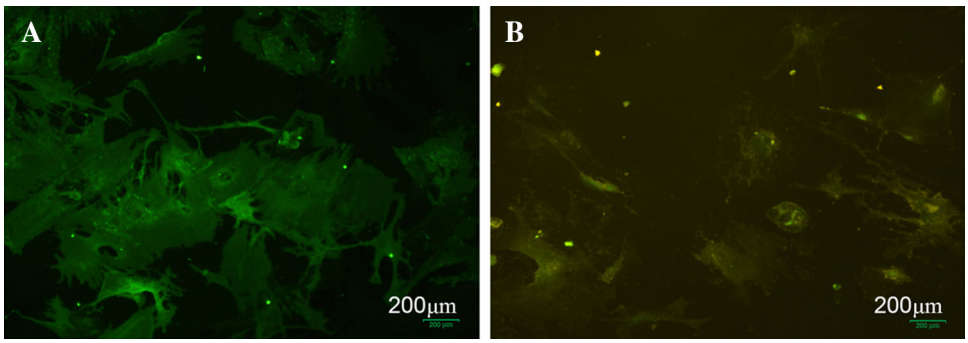

Fig. 5 Analysis of immunofluorescence staining. **a** CD44-PE cell marker fluoresced *green* on the surface. **b** CD34-PE cell marker fluoresced *brown*. *Scale bar* 200 μm, applies to all images

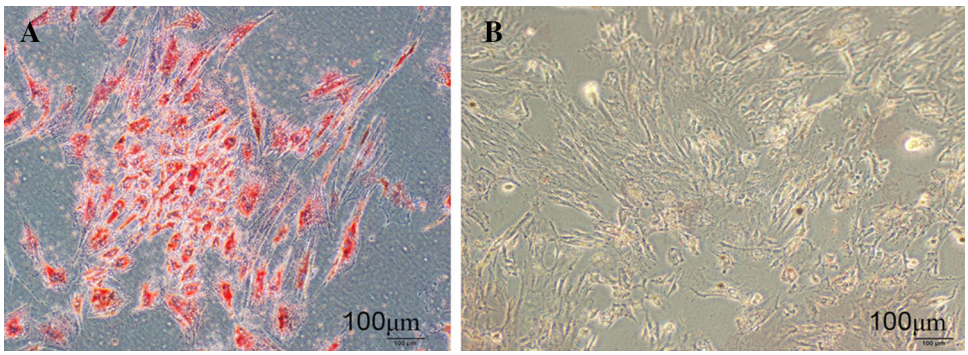

Fig. 6 Analysis of adipogenic induction. **a** Oil red O staining showed that the BMSCs were differentiated into adipocytes at day 10, obvious increase of cell mass was observed and cells were stained in bright red. **b** BMSCs were cultured in negative control medium. *Scale bar* 100 μm, applies to all images

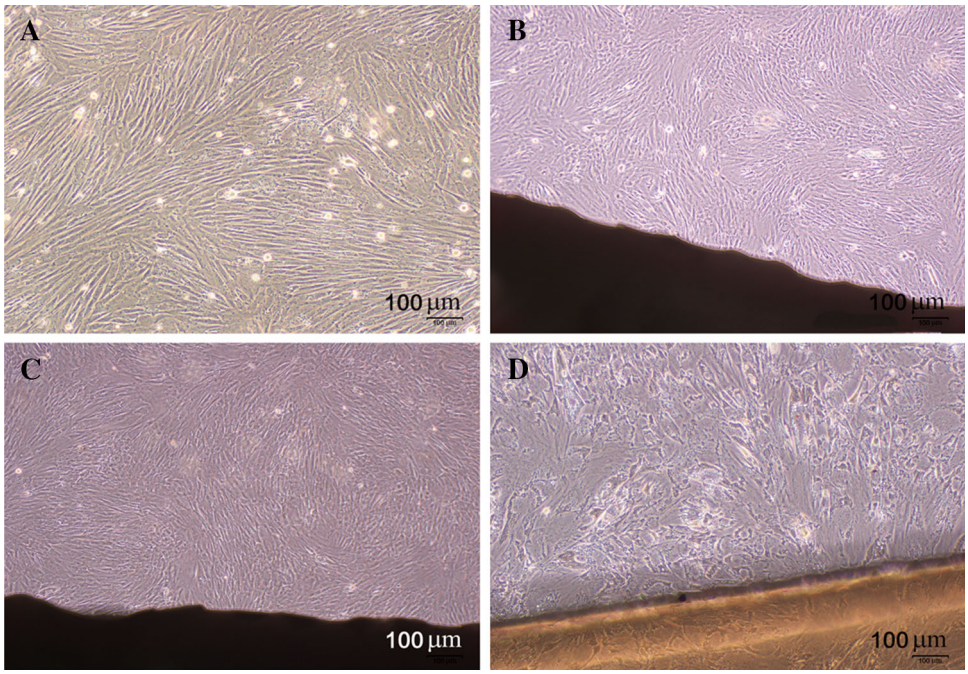

Fig. 7 Materials and BMSCs were co-cultured for 7 days. **a** Blank control group; **b** perfluoropropylene group; **c** 3DP tracheal graft group; **d** polyvinyl chloride group. *Scale bar* 100 μm, applies to all images

were positive for expressions of CD44 (Fig. 9a) and negative for CD34 (Fig. 9b), thus this confirmed the cells still were BMSCs.

Result of SRB

The proliferation of cells co-cultured with materials was analyzed with microplate reader (570 nm absorbance) at

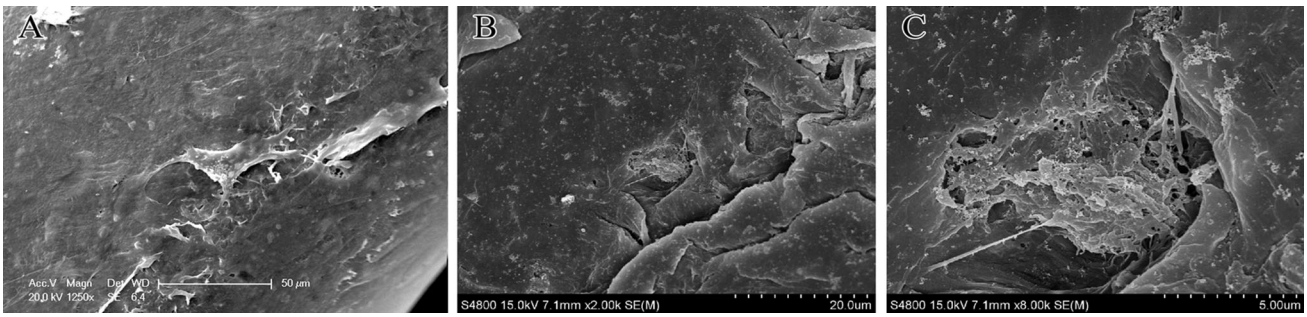

Fig. 8 SEM observation of co-cultured BMSCs. **a** BMSCs were found to attach onto the surface of 3DP tracheal graft using environmental scanning electron microscope (ESEM, ×1250); **b** BMSCs grew well inside the pores of the 3DP tracheal graft, as observed by field emission scanning electron microscopy (FESEM, ×2000); **c** ×8000

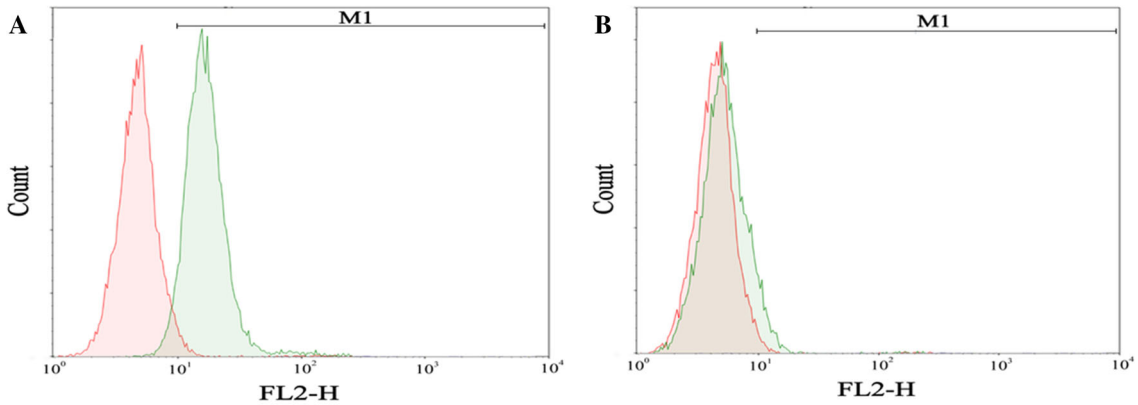

Fig. 9 Identification of the cells in 3DP racheal graft. The cells expressed the surface markers CD44 (**a**), but not CD34 (**b**), correspond to BMSCs

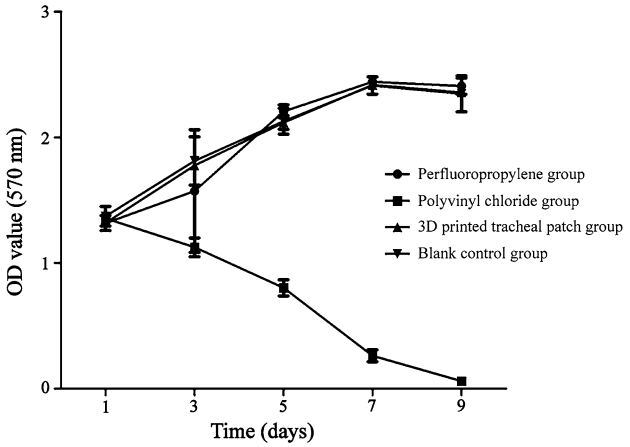

Fig. 10 Cell proliferation curves in different groups. BMSCs grew well on 3DP tracheal graft

days 1–9. As shown in Fig. 10, cell proliferation curves of the experimental group, the blank control group and negative control group were similar and had an "S" shape: all four groups of cells began to grow adherently at about 24 h, the curve of 1–7 days showed a trend of rising, and after 7 days started to decline due to cell death ($p > 0.05$, there was no statistically significant difference). While cell proliferation curve of the positive control group appeared a downward trend, and cells were almost all dead at day 7 ($p < 0.05$, there was statistically significant difference after day 1).

What's more, the collection of data for cell proliferation which were tested at 1, 7, 14, 21 days was shown in Fig. 11. The OD values for cells at 7, 14, 21 days were almost similar and the results demonstrated that 3DP tracheal graft had no influence on cell proliferation and possessed satisfactory biocompatibility.

Discussion and conclusion

Improvement of surgical techniques and immunosuppressive therapies after operation, combined with better immunological matching between donor and recipient, has enabled the success of organ transplantation [15]. Three-dimensional (3D) bioprinting has emerged as a new disruptive technology that may satisfy the ever-increasing demands of organ transplantation for offering many technical features [16]. 3D printing is a method that is derived

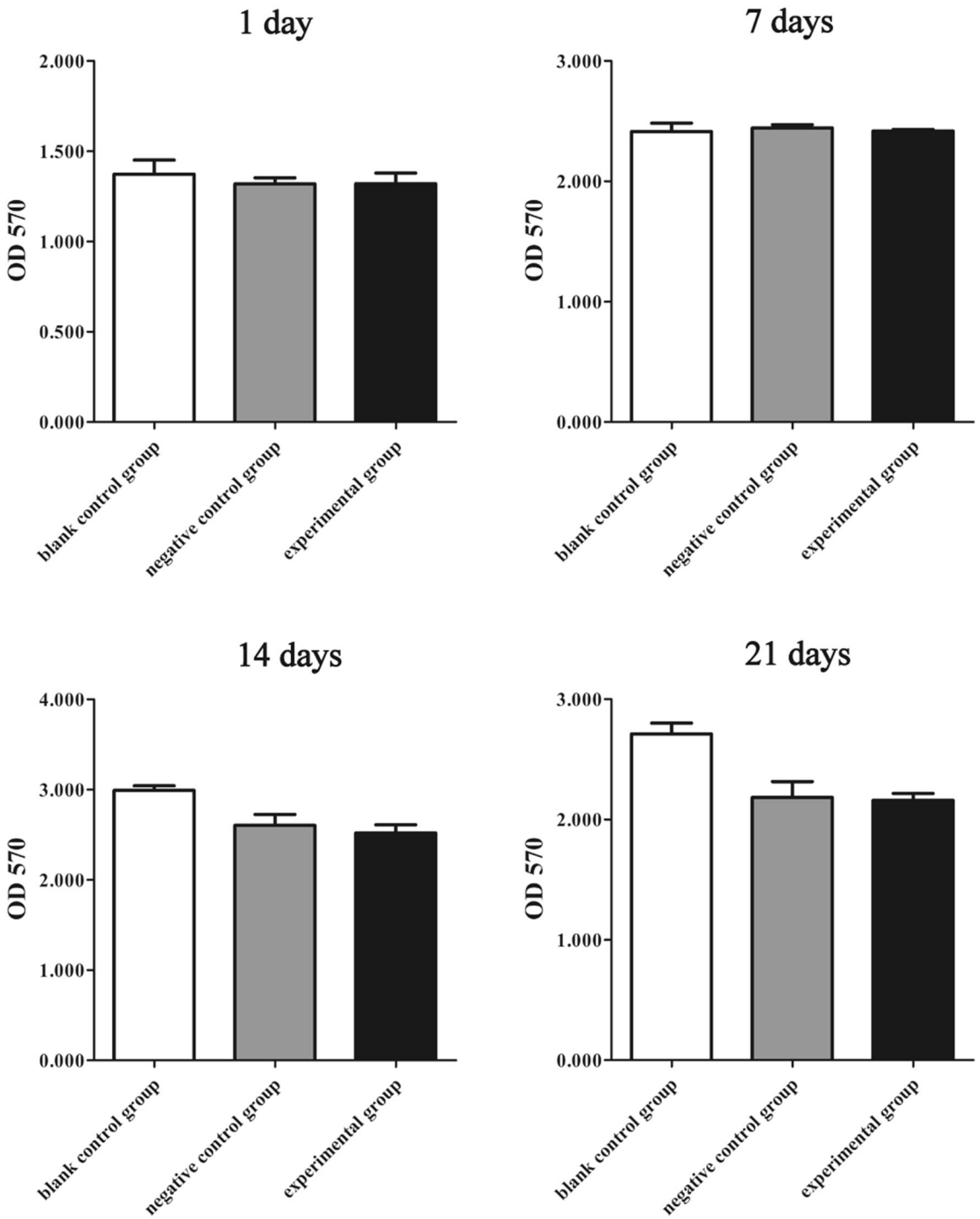

Fig. 11 Co-cultured for 21 days. The OD values for cells at 7, 14, 21 days were almost similar

from additive manufacturing technology. In a word, objects are fabricated by hierarchical processing forms which add materials layer by layer, hence rendering a three dimensional structure. The printed structures are designed using computer-aided-design (CAD) software that images are from computed tomography (CT), magnetic resonance imaging (MRI), or X-ray [17]. So, a 3D printing model of the damaged tissue or organ can be designed by mirroring the configuration of normal anatomy [11]. Compared with the traditional tissue engineering, 3D printing has the advantages of high precision, fast building, individual medical treatment and low immunological rejection [18]. Therefore, it is feasible to fabricate tracheal patch by 3D printing technology. Ideal biological scaffold should have

outstanding biological compatibility, can be degraded naturally and absorbed at the appropriate speed, last but not least, can provide micro-environment of differentiation for implanted cells [19]. Polycaprolactone (PCL) has the characteristics of good biological compatibility, excellent mechanical strength, durability, and thermoplasticity, also it has low melting point. These make PCL widely used in biological tissue engineering [20].

3D printing technology is emerging in recent years, whether the tracheal graft printed through the technology has excellent mechanical properties or good biocompatibility, all need to be analyzed by means of the experiments. The scaffold materials applied in tracheal tissue engineering must have considerable mechanical strength. Performing biomechanical test to evaluate mechanical behavior of 3D printed tracheal graft is necessary and reasonable. By this way, we can realize the predictability of mechanical properties in tracheal tissue engineering. The experimental results in this study showed that the 3DP graft has more excellent mechanical properties than native tracheal patch.

Nowadays, all biological materials must be tested via the experiments to estimate whether it has cytotoxicity [21]. The method of co-culturing with cells in vitro is the most commonly used [22]. Cell adhesion on the material is the basis of further cell growth and cell differentiation, it is also an important indicator to measure material biocompatibility. When the cells were cultured with toxic biological materials, the changes of the morphology, proliferation and adhesion condition provide the reliable evidence to assess the biocompatibility. In this study, 3DP tracheal graft and BMSCs were co-cultured, then cell morphology was observed, and the proliferation index of the cells on 3DP tracheal graft was quantified using SRB assay. The results showed that cell morphology of 3DP tracheal graft was normal at days 1–7, and was no significant difference with the blank control group and the negative control group; while cell pyknosis and vacuoles were observed in positive control group. At the same time, SRB results showed that cell proliferation curves of the experimental group, the blank control group and negative control group were similar and there was no statistically significant difference between them. While cell proliferation curve of the positive control group appeared a downward trend, and cells were almost all dead at day 7. These results adequately confirmed that the 3DP tracheal graft has no toxicity and good biocompatibility. What's more, the OD values for cells at 7, 14, 21 days were almost similar and the results demonstrated that 3DP tracheal graft had longer stability.

Our study was aimed at manufacturing tracheal graft for tracheal tissue engineering using PCL and 3D printing technology. Biomechanical and biocompatible test proved that 3DP tracheal graft was equipped with favorable cellular biocompatibility and biomechanical properties, in particular, the 3DP graft coated with BMSCs could be a promising implantable material for partial tracheal reconstruction.

Acknowledgements This study was supported by the National Natural Science Foundation of China (General Program 81170014, 81370118), High-end Talent Support Program of Yangzhou University (201431), Innovative program for postgraduate in Jiangsu Province (KYLX15_1388). The authors would like to thank the Qingdao Unique Products Develop Co., Ltd for fabrication of the 3D printed tracheal graft.

Compliance with ethical standards

Conflict of interest The authors declared no potential conflicts of interest with respect to the research, authorship, and/or publication of this article.

References

1. Park JH, Jung JW, Kang HW et al (2012) Development of a 3D bellows tracheal graft: mechanical behavior analysis, fabrication and an in vivo feasibility study. Biofabrication. doi:10.1088/1758-5082/4/3/035004
2. Svenja H, Katja SL (2013) Tracheal tissue engineering: building on a strong foundation. Expert Rev Med Devices 10:33–35
3. Wright CD, Grillo HC, Wain JC et al (2004) Anastomotic complications after tracheal resection: prognostic factors and management. J Thorac Cardiovasc Surg 128:731–739
4. Haag JC, Jungebluth P, Macchiarini P (2013) Tracheal replacement for primary tracheal cancer. Curr Opin Otolaryngol Head Neck Surg 21:171–177
5. Grillo HC (2002) Tracheal replacement: a critical review. Ann Thorac Surg 73:1995–2004
6. Elliott MJ, Haw MP, Jacobs JP et al (1996) Tracheal reconstruction in children using cadaveric homograft trachea. Eur J Cardiothorac Surg 10:707–712
7. Jungebluth P, Moll G, Baiguera S et al (2012) Tissue-engineered airway: a regenerative solution. Clin Pharmacol Ther 91:81–93
8. Kojima K, Vacanti CA (2014) Tissue engineering in the trachea. Anat Rec 297:44–50
9. Schantz JT, Teoh SH, Lim TC et al (2003) Repair of calvarial defects with customized tissue-engineered bone grafts I. Evaluation of osteogenesis in a three-dimensional culture system. Tissue Eng 9:S113–S126
10. Chang JW, Su AP, Park JK et al (2014) Tissue-engineered tracheal reconstruction using three-dimensionally printed artificial tracheal graft: preliminary report. Artif Organs 38:E95–E105
11. Seol YJ, Kang HW, Lee SJ et al (2014) Bioprinting technology and its applications. Eur J Cardiothorac Surg 46:342–348
12. Mäkitie AA, Korpela J, Elomaa L et al (2013) Novel additive manufactured scaffolds for tissue engineered trachea research. Acta Otolaryngol 133:412–417
13. Berndt-Weis ML, Kauri LM, Williams A et al (2009) Global transcriptional characterization of a mouse pulmonary epithelial cell line for use in genetic toxicology. Toxicol In Vitro 23:816–833
14. Zhang W, Zhang F, Shi H et al (2014) Comparisons of rabbit bone marrow mesenchymal stem cell isolation and culture methods in vitro. PLoS One. doi:10.1371/journal.pone.0088794

15. Abecassis M, Adams M, Adams P et al (2000) Consensus statement on the live organ donor. JAMA 284:2919–2926
16. Yoo SS (2015) 3D-printed biological organs: medical potential and patenting opportunity. Expert Opin Ther Pat 25:507–511
17. Obregon F, Vaquette C, Ivanovski S et al (2015) Three-dimensional bioprinting for regenerative dentistry and craniofacial tissue engineering. J Dent Res 94:143S–152S
18. Shi J, Zhong YM (2014) Three-dimensional bioprinting technology in tissue engineering. Chin J Tissue Eng Res 18:271–276
19. Zhou K, Zhou XM (2006) Tissue engineering heart valve and the prospect of stem cells for tissue engineering application. Int J Biomed Eng 29:110–113
20. Lefebvre F, David C, Wauven CV (2001) Biodegradation of polycaprolactone by micro-organisms from an industrial compost of household refuse. Polym Eng Sci 41:727
21. Alexander F, Franz KN, Astrid S et al (2007) Cytotoxicity of resin composites as a function of interface area. Dental Mater 23:1438–1446
22. Burt HM, Zhang X, Toleikis P et al (1999) Development of copolymers of poly(D, l-lactide) and methoxypolyethylene glycol as micellar carriers of paclitaxel. Colloids Surf B Biointerfaces 16:161–171